Expression pattern of class I phosphoinositide 3-kinase and distribution of its product, phosphatidylinositol-3, 4, 5-trisphosphate, during *Drosophila* embryogenesis

ショウジョウバエの胚発生におけるクラスI ホスホイノシチド3-キナーゼ及びその産物、ホスファチジルイノシトール-3,4,5-三リン酸の発現パターン

指導教員　和泉　孝志 教授

平成 26 年 1 月

群馬大学医学系研究科

平成 22 年入学

代謝機能制御系・生化学

郗 昕

Contents

Abbreviations

CL: cardiolipin

Chl: cholesterol

CMW: mixed solvent of chloroform: methanol: water = 65: 35: 8.

DG: diacylglycerol

PA: phosphatidic acid

PC: phosphatidylcholine

PE: phosphatidylethanolamine

PG: phosphatidylglycerol

PI: phosphatidylinositol

PI3K: phosphoinositide 3-kinase

PIP: phosphatidylinositol phosphate

PIP_2: phosphatidylinositol-bisphosphate

PIP_3: phosphatidylinositol 3, 4, 5-trisphosphate

PS: phosphatidylserine

SM: sphingomyelin

TG: triglyceride

Introduction

Phosphoinositide 3-kinases (PI3Ks) phosphorylate inositol lipids at the 3' position of the inositol ring to generate lipids at the plasma membrane. These phosphorylated lipids are important for many cellular functions, such as cell growth, proliferation, differentiation, motility, survival and intracellular trafficking (Wymann and Pirola, 1998; Cantley, 2002). The PI3K family is divided into three classes: class I, class II, and class III. *Drosophila* possesses a single PI3K from each class (MacDougall et al., 1995). Class I PI3Ks phosphorylate PI, PI(4)P and $PI(4,5)P_2$ to generate PI(3)P, $PI(3,4)P_2$ and $PI(3,4,5)P_3$, respectively. In *Drosophila*, the class I PI3Ks contain a regulatory subunit p60 and a catalytic p110 subunit. Class II PI3Ks phosphorylate PI and PI(4)P. Class II kinases are monomeric and possess a C-terminal C2 domain. Class III PI3Ks only phosphorylate PI to generate PI(3)P. Class III kinases contain a Vps34 catalytic subunit and a Vps15/p150 regulatory subunit (Domin and, Waterfield, 1997; Wymann and Pirola, 1998; Foster et al., 2003).

Class I PI3Ks can be activated by a large variety of extracellular stimuli and are responsible for generating $PI(3,4,5)P_3$ from $PI(4,5)P_2$ at the plasma membrane. They have diverse roles in development, actin rearrangement, modification of intracellular membranes, cell size, motility, survival and proliferation (Fry, 2001; Katso et al., 2001; Brachmann et al., 2005). The regulatory subunit of *Drosophila* class I PI3Ks, p60, includes two SH2 domains and an inter-SH2 domain. The p60 has a short N-terminus and a unique C- terminus of 70 amino acids that shows no significant similarity to other proteins (Weinkove et al., 1997). The expression pattern of *Pi3K21B*, encoding *Drosophila* p60 regulatory subunit, has been investigated during embryogenesis by *in*

situ hybridization. *Pi3K21B* are ubiquitously distributed in preblastoderm embryos and are degraded during blastoderm formation. After cellularblastoderm the transcripts are found specifically in the pole cells, and sustain during germ band elongation (Albert et al., 1997). The catalytic subunit of *Drosophila* class I PI3K, Dp110, contains catalytic core (HR1) and PIK domain (HR2) at the C-terminus. It forms a heterodimer with regulatory subunit p60. The Dp110/p60 complex possesses PI3K activity and controls growth during imaginal disc development. Ectopic Dp110 expression affects both growth and organization in the eye and the wing (Leevers et al., 1996; Weinkove et al., 1997). Class I PI3Ks require both catalytic and regulatory subunits to generate $PI(3,4,5)P_3$ and exert their effects.

In *Drosophila*, embryogenesis begins with 13 nuclei divisions generating some 6000 nuclei that are located just beneath the plasma membrane. Cellularization then begins, resulting in the formation of lateral and then basal membranes around each nucleus. At the end of cellularization, all somatic cells are columnar and their nuclei locate apically (Turner and Mahowald, 1976). Gastrulation begins with the formation of the ventral furrow. Shortly after the ventral furrow begins to form, invagination of posterior midgut primodium starts at the posterior region. The initial invaginations of both the ventral furrow and posterior endoderm primordium have similar cell shape changes. They first flatten on their apical sides and progressively constrict their apical sides, resulting in elongation of the cells and displacement of the nuclei basally. This apical constriction generates a force that pulls neighboring cells towards the area of constriction, producing a shallow groove. The cells then shorten and expand their basal ends, which generates the force that causes the initial groove to invaginate (Brownes, 1975; Turner and

Mahowald, 1977; Leptin and Grunewald, 1990; Sweeton et al., 1991). Forces that drive apical constriction are generated by contraction of an actin filament (F-actin) network via the molecular motor non-muscle myosin II (Hildebrand, 2005; Kasza and Zallen, 2011; Lecuit et al., 2011; Young et al., 1991; Martin et al., 2009).

The expression pattern of *Pi3K21B*, encoding the *Drosophila* p60 regulatory subunit of the Class I PI3Ks, has been investigated during embryogenesis by *in situ* hybridization (Albert et al., 1997). However, the expression pattern of *Drosophila Pi3K92E* encoding the p110 catalytic subunit in embryogenesis has not yet been reported. In this study, we examined the expression pattern of *Pi3K21B, Pi3K92E* and the distribution of $PI(3,4,5)P_3$, the enzymatic product of the Class I PI3Ks, during *Drosophila* embryogenesis.

Materials and Methods

Transgenic flies

The tGPH strain was obtained from the Bloomington Drosophila Stock Center (Bloomington, IN). The transgenic EGFP flies expressed EGFP driven by the tubulin promoter were generated by P-element-mediated transformation.

Whole-mount *in situ* hybridization

Whole-mount *in situ* hybridization was prepared according to Tautz and Pfeifle (1989). Embryos were dechorionated and fixed in a 1:1 mixture of heptane and fixation buffer containing 4% formaldehyde for 25 min with vigorously shaking. After devitellinization in methanol, embryos were rinsed 6 times in ethanol for total 1 hr. Rock the embryos in 50/50 xylenes/ethanol for 30 min. After rinse 5 times in ethanol and twice in methanol, the embryos were incubated with rocking for 5 min in 50/50 methanol/ PBT+5% formaldehyde. Then incubate them with rocking for 25 min in PBT+5% formaldehyde. After rinse 5 times in PBT, they were incubated with rocking for 2-3 min in PBT containing 4μg/ml Proteinase K. After removing Proteinase K, embryos were fixed again in PBT/5% formaldehyde for 25 min. Then pre-hybridize for 1hr in 1ml hybridization solution at 55℃. Full-length cDNA clones, LD42724 for *Pi3K21B* and SD05105 for *Pi3K92E*, were used for preparing RNA probes. The probes were digoxigenin-labeled by *in vitro* transcription using T7 or SP6 RNA polymerase.

Protein lipid overlay assay

GST-fusion proteins were prepared by cloning PH domain of GRP1 into pGEX6P-1 vector (GE Healthcare, UK). One hundred pmol of the lipid samples were spotted on a Hybond-C Extra membrane (GE Healthcare, UK). After drying for 1 h at room temperature, the membrane was incubated in blocking buffer (PBS/0.1% Tween20/1% fatty acid free BSA) with gentle rocking for 1 h. The membrane was then incubated at room temperature for 1 h with gentle rocking in fresh blocking buffer containing 5 nM GST-fusion proteins. After five washes of 5 min in PBST, the membrane was incubated for 1 h at room temperature with anti-GST (goat anti-GST, GE Healthcare, UK) at 1/2000 dilution in blocking buffer, followed by incubation with secondary antibody of anti-goat IgG-HRP at 1/5000 dilution in blocking buffer. Binding was detected by the ECL plus kit (GE Healthcare, UK) (Dowler et al., 2002).

Embryo fixation, immuno-staining and confocal imaging

Embryos were dechorionated and fixed in a 1:1 mixture of heptane and buffer B (10 mM KPO_4 pH 6.8, 15 mM NaCl, 45 mM KCl, 2 mM $MgCl_2$) containing 4% formaldehyde. After devitellinization in methanol or 80% ethanol (for phalloidin staining), embryos were incubated in blocking solution (in 1% BSA in PBS). Embryos were incubated with primary antibody followed by secondary antibody, and mounted in 50% glycerol in PBS. Primary antibody was diluted as follows: anti-GFP (Clontech, CA) 1:100, anti-Vasa 0.5 μg/ml. For F-actin staining, 1:50 diluted phalloidin conjugated with Alexa546 (Molecular Probes, OR) was used. For nuclear staining, 1:2000 diluted SYTOX Orange (Molecular Probes, OR) was used. Confocal images of immuno-stained embryos were obtained using LSM 510 (Carl Zeiss, Germany). Image analyses were performed using LSM Image Browser (Carl Zeiss, Germany).

Results

Expression pattern of class I *Pi3K* RNA

The expression pattern of *Drosophila* class I *Pi3K21B* and *Pi3K92E* was examined by *in situ* hybridization during *Drosophila* embryogenesis (Fig. 1 and 2). *Pi3K21B* encodes the p60 adaptor (Albert et al., 1997), and *Pi3K92E* encodes Dp110 (Leevers et al., 1996). The Dp110 and p60 complex possesses both lipid and protein kinase activity (Weinkove et al., 1997). *Pi3K21B* was expressed maternally and became stronger at the posterior of the embryos (Fig. 1A-C). It was expressed primarily in pole cells after cellularization and sustained during germ band elongation (Fig. 1D-H). During late embryogenesis, *Pi3K21B* was expressed ubiquitously (Fig. 1I-K). Our results are consistent with Albert et al. (1997). *Pi3K92E* was expressed maternally before cellularization (Fig. 2A and B), after which its expression level decreased. A faint signal was observed at the posterior of the cellularizing embryo (Fig. 2C). At the start of gastrulation, a slightly stronger signal was observed along the ventral furrow (Fig. 2D and F) and posterior midgut primordium (Fig. 2E and G). The *Pi3K92E* RNA was also slightly accumulated in dorsal furrows (Fig.2H). In later stages, expression became ubiquitous after germ band elongation and persisted during germ band shortening (Fig. 2I-L). The *Pi3K21B* transcript was rarely detected during gastrulation, but a stronger signal of *Pi3K92E* RNA was observed along the ventral furrow and posterior midgut primordium during gastrulation.

GRP1-PH specifically binds PI(3,4,5)P_3

To investigate whether the catalytic function of PI3K is active during gastrulation, we employed an *in vivo* approach to examine the distribution of its product, $PI(3,4,5)P_3$.

The PH domain from GRP1, a guanine nucleotide exchange factor for small GTPases of the ARF family, was reported to bind with high affinity and selectivity to $PI(3,4,5)P_3$ *in vitro* (Kavran et al., 1998). We tested the binding specificity of GRP1-PH by a protein lipid overlay assay using GST-fusion lipid-binding proteins. Protein bound to lipid was detected by anti-GST antibody. As expected, GRP1-PH bound $PI(3,4,5)P_3$ with high affinity (Fig. 3A). The negative control GST did not bind any of the lipids (Fig. 3B).

$PI(3,4,5)P_3$ accumulates at the apical region of the cells undergoing invagination during *Drosophila* gastrulation

Next, transgenic tGPH flies that encode the EGFP-GRP1-PH domain were used to visualize the distribution of $PI(3,4,5)P_3$ (Britton et al., 2002). The embryos were double stained with anti-GFP and anti-Vasa antibodies to identify the pole cells or SYTOX Orange to identify the nucleus (Fig. 4). In stage 6, the cells of the posterior midgut primordium were undergoing invagination. $PI(3,4,5)P_3$ was found to distribute at the apical and lateral region of the invaginating cells and a stronger signal accumulated at the apical region of these cells (Fig. 4A, B and E). The negative control EGFP showed uniform staining pattern (Fig. 4C, D and F). During ventral furrow formation, $PI(3,4,5)P_3$ also accumulated at the apical region of the invaginating ventral cells (Fig. 5A and B), whereas the negative control EGFP showed uniform staining (Fig. 5C and D). Regulation of invagination during *Drosophila* gastrulation is a paradigm for how

signal transduction directs morphogenesis. The actomyosin networks that drive invagination are regulated by Fog-depended signaling to activate non-muscle myosin II and Fog-independent organization of cortical F-actin (Sawyer et al., 2010). We found a slightly stronger signal of PI(3,4,5)P_3 at the apical region of the cells undergoing invagination. To investigate the relationship between PI(3,4,5)P_3 and the actomyosin network, we next examined the distribution of PI(3,4,5)P_3 and F-actin.

The distribution of PI(3,4,5)P_3 partially matches that of F-actin during invagination

The embryos were double stained with anti-GFP for EGFP-GRP1-PH and phalloidin for F-actin. During posterior midgut invagination, PI(3,4,5)P_3 was found to distribute at the apical and lateral region of the invaginating cells and a stronger signal accumulated at the apical region of these cells where actin also accumulated (Fig. 6A and B). The negative control EGFP showed uniform staining pattern (Fig. 6C and D). During ventral furrow formation, PI(3,4,5)P_3 was also found to accumulate at the apical region of the invaginating (Fig. 7A and B) and invaginated (Fig. 7C and D) ventral cells where actin also accumulated, whereas the negative control EGFP showed uniform staining pattern (Fig. 7E–H).

Discussion

We showed that *Pi3K21B* expressed maternally and primarily in pole cells after cellularization until completion of germ band elongation, consistent with previous results (Albert et al., 1997). We also examined expression pattern of the catalytic subunit of class Ⅰ PI3K, *Pi3K92E*, showing that it also expressed maternally. At the start of gastrulation, a slightly stronger signal was observed along the ventral furrow and posterior midgut primordium. Even *Pi3K21B* expressed primarily in pole cells during this period, the proteins may be exist longer than RNA. To invesgigate whether the catalytic function of PI3K exsits during gastrulation, we examined the distribution of its pruduct PI(3,4,5)P_3 *in vivo* using the lipid specific binding protein. We found that PI(3,4,5)P_3 accumulates at the apical of the cells that undergo invagination during *Drosophila* gastrulation and partially matches that of F-actin. It may suggest a potential involvement of PI(3,4,5)P_3 in the regulation of the actomyosin network. PI(3,4,5)P_3 is the product of class I PI3Ks, and both have important roles in cytoskeleton regulation. In *Drosophila* cultured S2R+ cells, PI3K signaling controls cortical actin organization (Jovceva et al., 2007). At the immunological synapse formed by T-lymphocytes, remodeling of the F-actin ring is dictated by the accumulation of PI(3,4,5)P_3 that is generated by class I PI3Ks (Le Floc'h et al., 2013). This raises the exciting possibility that class I PI3Ks and PI(3,4,5)P_3 may have a similar role in the regulation of actin polymerization during *Drosophila* gastrulation. PI(3,4,5)P_3, as a lipid second messenger, activates a variety of downstream molecules by binding to their pleckstrin-homology (PH) domains (DiNitto et al., 2003). During *Drosophila* gastrulation, RhoGEF2, which possesses a PH domain, regulates both F-actin and myosin accumulation (Barrett et al.,

1997; Fox and Peifer, 2007; Kolsch et al., 2007). Together, this suggests a possibility for PI(3,4,5)P_3 to be involved in the regulation of the actomyosin network during invagination in *Drosophila* gastrulation.

Summary

The class I phosphoinositide 3-kinase (PI3K) can be activated by a large variety of extracellular stimuli and is responsible for generating phosphatidylinositol-3, 4, 5-trisphosphate (PI(3,4,5)P_3) from phosphatidylinositol-4, 5-bisphosphate at the plasma membrane. The expression pattern of the class I PI3K and distribution of PI(3,4,5)P_3, visualized by its specific binding protein, GRP1-PH, were examined during *Drosophila* embryogenesis. We found that the RNA of *Pi3K21B*, encoding the *Drosophila* p60 regulatory subunit of the Class I PI3Ks, was expressed maternally and expressed primarily in pole cells after cellularization until completion of germ band elongation. The RNA of *Pi3K92E*, encoding the *Drosophila* p110 catalytic subunit of the Class I PI3Ks, was also expressed maternally. During gastrulation, its transcript level became lower and was slightly enriched in invaginating cells. Both *Pi3K21B* and *Pi3K92E* were expressed ubiquitously after germ band elongation and persisted during germ band shortening. PI(3,4,5)P_3 was distributed at the apical region of the invaginating cells during gastrulation. These findings suggest a possible involvement of class I PI3K and PI(3,4,5)P_3 in the regulation of invagination during gastrulation.

References

Albert, S., Twardzik, T., Heisenberg, M., Schneuwly, S., 1997. Isolation and characterization of the *droPIK57* gene encoding a new regulatory subunit of phosphatidylinositol 3-kinase from *Drosophila melanogaster*. Gene **198**, 181-189.

Barrett, K., Leptin, M., Settleman, J., 1997. The Rho GTPase and a putative RhoGEF mediate a signaling pathway for the cell shape changes in *Drosophila* gastrulation. Cell **91**, 905–915.

Bownes M., 1975. A photographic study of development in the living embryo of *Drosophila melanogaster*. J. Embryol. Exp. Morphol. **33**, 789-801.

Brachmann, S.M., Yballe, C.M., Innocenti, M., Deane, J.A., Fruman, D.A, Thomas, S.M., 2005. Cantley LC. Role of phosphoinositide 3-kinase regulatory isoforms in development and actin rearrangement. Mol. Cell. Biol. **25**, 2593-2606.

Britton, J.S., Lockwood, W.K., Li, L., Cohen, S.M., Edgar, B.A., 2002. *Drosophila*'s insulin/PI3-kinase pathway coordinates cellular metabolism with nutritional conditions. Dev. Cell. **2**, 239-249.

Cantley, L. C., 2002. The phosphoinositide 3-kinase pathway. Science **296**, 1655–1657.

Costa, M., Wilson, E., Wieschaus, E., 1994. A putative cell signal encoded by the folded gastrulation gene coordinates cell shape changes during *Drosophila* gastrulation. Cell **76**, 1075–1089.

DiNitto, J.P., Cronin T.C., Lambright D.G., 2003. Membrane recognition and targeting by lipid-binding domains. Sci. STKE. re16.

Domin, J., Waterfield, M.D., 1997. Using structure to define the function of phosphoinositide 3-kinase family members. FEBS Lett. **410**, 91-95.

Dowler, S., Kular, G., Alessi, D.R., 2002. Protein lipid overlay assay. Sci. STKE. pl6.

Foster, F.M., Traer, C.J., Abraham, S.M., Fry, M.J., 2003. The phosphoinositide (PI) 3-kinase family. J. Cell Sci. **116**, 3037-3040.

Fox, D.T., Peifer, M., 2007. Abelson kinase (Abl) and RhoGEF2 regulate actin organization during cell constriction in *Drosophila*. Development **134**, 567–578.

Fry, M.J., 2001. Phosphoinositide 3-kinase signalling in breast cancer: how big a role might it play? Breast Cancer Res. **3**,304-312.

Hildebrand, J. D., 2005. Shroom regulates epithelial cell shape via the apical positioning of an actomyosin network. J. Cell Sci. **118**, 5191–5203.

Homem, C.C., Peifer, M., 2008. Diaphanous regulates myosin and adherens junctions to control cell contractility and protrusive behavior during morphogenesis. Development **135**, 1005–1018.

Jovceva, E., Larsen, M.R., Waterfield, M.D., Baum, B., Timms, J.F., 2007. Dynamic cofilin phosphorylation in the control of lamellipodial actin homeostasis. J. Cell Sci. **120**,1888-1897.

Kasza, K.E., Zallen, J.A., 2011. Dynamics and regulation of contractile actin-myosin networks in morphogenesis. Curr. Opin. Cell Biol. **23**, 30–38.

Katso, R., Okkenhaug, K., Ahmadi, K., White, S., Timms, J., 2001. Cellular function of phosphoinositide 3-kinases: implications for development, homeostasis, and cancer. Annu. Rev. Cell Dev. Biol. **17**, 615–675.

Kavran, J.M., Klein, D.E., Lee, A., Falasca, M., Isakoff, S.J., Skolnik, E.Y. and Lemmon, M.A. 1998. Specificity and promiscuity in phosphoinositide binding by pleckstrin homology domains. J. Biol. Chem. **273**, 30497–30508

Kolsch, V., Seher, T., Fernandez-Ballester, G.J., Serrano, L., Leptin, M., 2007. Control of *Drosophila* gastrulation by apical localization of adherens junctions and RhoGEF2. Science. **315**, 384-386.

Le, Floc'h A., Tanaka, Y., Bantilan, N.S., Voisinne, G., Altan-Bonnet, G., Fukui, Y., Huse, M., 2013. Annular PIP3 accumulation controls actin architecture and modulates cytotoxicity at the immunological synapse. J. Exp. Med. **210**, 2721-2737.

Lecuit, T., Lenne, P. F. & Munro, E., 2011. Force generation, transmission, and integration during cell and tissue morphogenesis. Annu. Rev. Cell Dev. Biol. **27**, 157–184.

Leevers, S.J., Weinkove, D., MacDougall, L.K., Hafen, E., Waterfield, M.D., 1996. The *Drosophila* phosphoinositide 3-kinase Dp110 promotes cell growth. EMBO J. **15**, 6584-6594.

Leptin, M., Grunewald, B., 1990. Cell shape changes during gastrulation in *Drosophila*. Development **110**, 73–84.

MacDougall, L.K., Domin, J., Waterfield, M.D., 1995. A family of phosphoinositide 3-kinases in *Drosophila* identifies a new mediator of signal transduction. Curr. Biol. **5**, 1404-1415.

Martin, A.C., Kaschube, M., Wieschaus, E.F.. 2009. Pulsed contractions of an actin-myosin network drive apical constriction. Nature. **457**, 495-499.

Morize, P., Christiansen, A.E., Costa, M., Parks, S., Wieschaus, E., 1998. Hyperactivation of the folded gastrulation pathway induces specific cell shape changes. Development **125**, 589–597.

Nikolaidou, K.K., Barrett, K., 2004. A Rho GTPase signaling pathway is used reiteratively in epithelial folding and potentially selects the outcome of Rho activation. Curr. Biol. **14**, 1822–1826.

Parks, S., Wieschaus, E., 1991. The *Drosophila* gastrulation gene *concertina* encodes a G alpha-like protein. Cell **64**, 447-458.

Rogers, S.L., Wiedemann, U., Hacker, U., Turck, C., Vale, R.D., 2004. *Drosophila* RhoGEF2 associates with microtubule plus ends in an EB1-dependent manner. Curr. Biol. **14**, 1827–1833.

Sawyer, J.M., Harrell, J.R., Shemer, G., Sullivan-Brown, J., Roh-Johnson, M., Goldstein, B., 2010. Apical constriction: a cell shape change that can drive morphogenesis. Dev Biol. **341**, 5-19.

Sweeton,D., Parks,S., Costa,M. and Wieschaus,E., 1991. Gastrulation in *Drosophila*: the formation of the ventral furrow and posterior midgut invaginations. Development **112**, 775–789.

Tautz, D., Pfeifle, C., 1989. A non-radioactive *in situ* hybridization method for the localization of specific RNAs in *Drosophila* embryos reveals translational control of the segmentation gene *hunchback*. Chromosoma. **98**, 81-85.

Turner, F.R., Mahowald, A.P., 1976. Scanning electron microscopy of Drosophila embryogenesis. 1. The structure of the egg envelopes and the formation of the cellular blastoderm. Dev. Biol. **50**, 95-108.

Turner, F.R., Mahowald, A.P., 1977. Scanning electron microscopy of *Drosophila* melanogaster embryogenesis II. Gastrulation and segmentation. Dev. Biol. **57**, 403-416.

Weinkove, D., Leevers, S.J., MacDougall, L.K., Waterfield, M.D., 1997. p60 is an adaptor for the *Drosophila* phosphoinositide 3-kinase, Dp110. J. Biol. Chem. **272**, 14606-14610.

Wymann, M.P., Pirola, L., 1998. Structure and function of phosphoinositide 3-kinases. Biochim. Biophys. Acta. **1436**, 127-150.

Young, P.E., Pesacreta, T.C., Kiehart, D.P., 1991. Dynamic changes in the distribution of cytoplasmic myosin during *Drosophila* embryogenesis. Development **111**, 1–14.

Zusman, S.B., Wieschaus, E.F., 1985. Requirements for zygotic gene activity during gastrulation in *Drosophila* melanogaster. Dev. Biol. **111**, 359–371.

Figure legends

Fig. 1 Expression pattern of *Pi3K21B* RNA

Expression pattern of *Pi3K21B* was examined by *in situ* hybridization throughout *Drosophila* embryogenesis. Embryonic stage (st.) is indicated. (A–C) *Pi3K21B* was expressed maternally before cellularization and a stronger signal was observed at the posterior of the embryos. (D–H) *Pi3K21B* was expressed primarily in pole cells (arrows). (I-K) *Pi3K21B* was expressed ubiquitously.

Fig. 2 Expression pattern of *Pi3K92E* RNA

Expression pattern of *Pi3K92E* was examined by *in situ* hybridization throughout *Drosophila* embryogenesis. Embryonic stage (st.) is indicated. (A and B) *Pi3K92E* was expressed maternally before cellularization. (C) *Pi3K92E* expression level was decreased in the cellular blastoderm. A faint signal was observed at the posterior of the cellularizing embryo. (D) Ventral view of a stage 6 embryo during gastrulation. *Pi3K92E* was expressed along the ventral furrow. (E) Lateral view of stage 6 embryo during gastrulation. *Pi3K92E* was expressed slightly stronger at the invaginating cells of posterior midgut invagination. (F and G) High magnification of D and E. Arrows indicate *Pi3K92E* was expressed along the ventral furrow and invaginating cells of posterior midgut invagination. (H) *Pi3K92E* was expressed slightly stronger in dorsal furrows. (I-L) During late embryogenesis *Pi3K92E* was expressed ubiquitously.

Fig. 3 Binding specificity of GST-lipid-binding domain for various lipids

The binding specificity of GRP1-PH was examined by a protein lipid overlay assay using GST-fused proteins. Protein bound to lipid was detected by anti-GST antibody. (A) GST-GRP1-PH mainly binds PI(3,4,5)P_3. (B) Negative control GST does not bind any of the lipids. (C) The layout diagram of the various lipids.

Fig. 4 PI(3,4,5)P_3 accumulates at the apical region of the cell during posterior midgut invagination

(A–D) Embryos were double stained with anti-GFP (green) for EGFP-GRP1-PH and anti-Vasa (red) for pole cells. (E and F) Embryos were double stained with anti-GFP (green) for EGFP-GRP1-PH and SYTOX Orange (red) for nucleus. (A, B, E) Transgenic line of EGFP-GRP1-PH. (C, D, F) Transgenic line of EGFP. (A, C, E) One section of lateral view of the posterior. (B, D) 3D view of the posterior. Arrows indicate PI(3,4,5)P_3 accumulation at the apical region of the cell undergoing invagination.

Fig. 5 PI(3,4,5)P_3 accumulates at the apical region of the cell during ventral furrow formation

Embryos were double stained with anti-GFP (green) for EGFP-GRP1-PH and SYTOX Orange (red) for nucleus. (A and B) Transgenic line of EGFP-GRP1-PH. (C and D) Transgenic line of EGFP. (A and C) Ventral view of the ventral furrow surface at the beginning of invagination. (B and D) Ventral view of the invaginated cells of the ventral furrow. Arrows indicate PI(3,4,5)P_3 accumulation at the apical region of the cell undergoing invagination.

Fig. 6 Subcellular distribution of PI(3,4,5)P_3 and F-actin during posterior midgut invagination

Embryos were double stained with anti-GFP (green) and phalloidin (red) for F-actin. (A and B) Transgenic line of EGFP-GRP1-PH. (C and D) Transgenic line of EGFP. (A, C) One section of lateral view of the posterior. (B, D) 3D view of the posterior. Arrows indicate PI(3,4,5)P_3 accumulation at the apical region of the cell undergoing invagination.

Fig. 7 Subcellular distribution of PI(3,4,5)P_3 and F-actin during ventral furrow formation

Embryos were double stained with anti-GFP (green) and phalloidin (red) for F-actin. (A–D) Transgenic line of EGFP-GRP1-PH. (E-H) Transgenic line of EGFP. (A and E) Ventral view of the ventral furrow surface at the beginning of invagination. (B and F) Cross section of the ventral furrow surface at the beginning of invagination. (C and G) Ventral view of the invaginated cells of the ventral furrow. (D and H) Cross section of the ventral furrow at the stage that invagination was completed. Arrows indicate PI(3,4,5)P_3 accumulated at the apical of the cell undergoing invagination and fully invaginated.

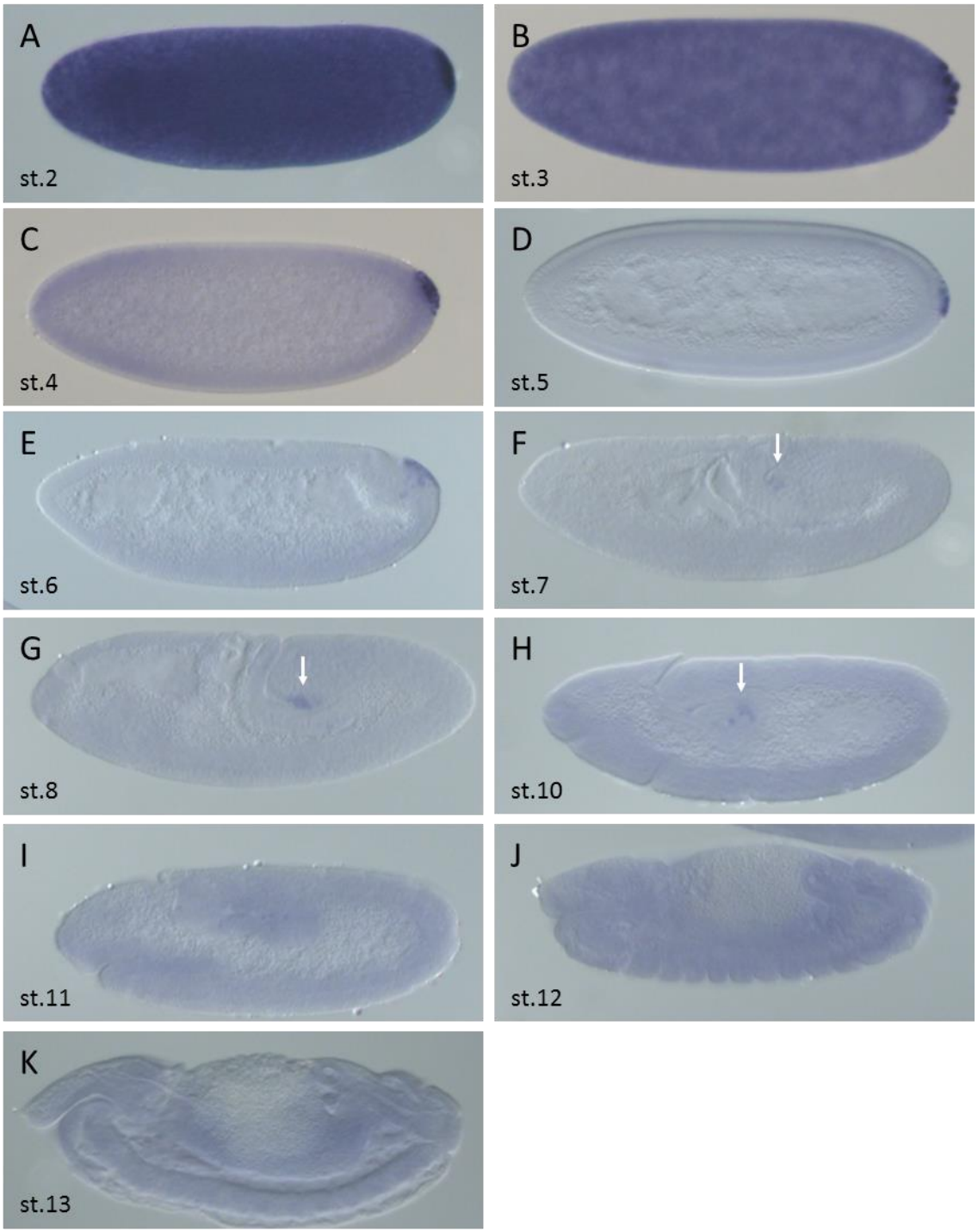

Fig.1

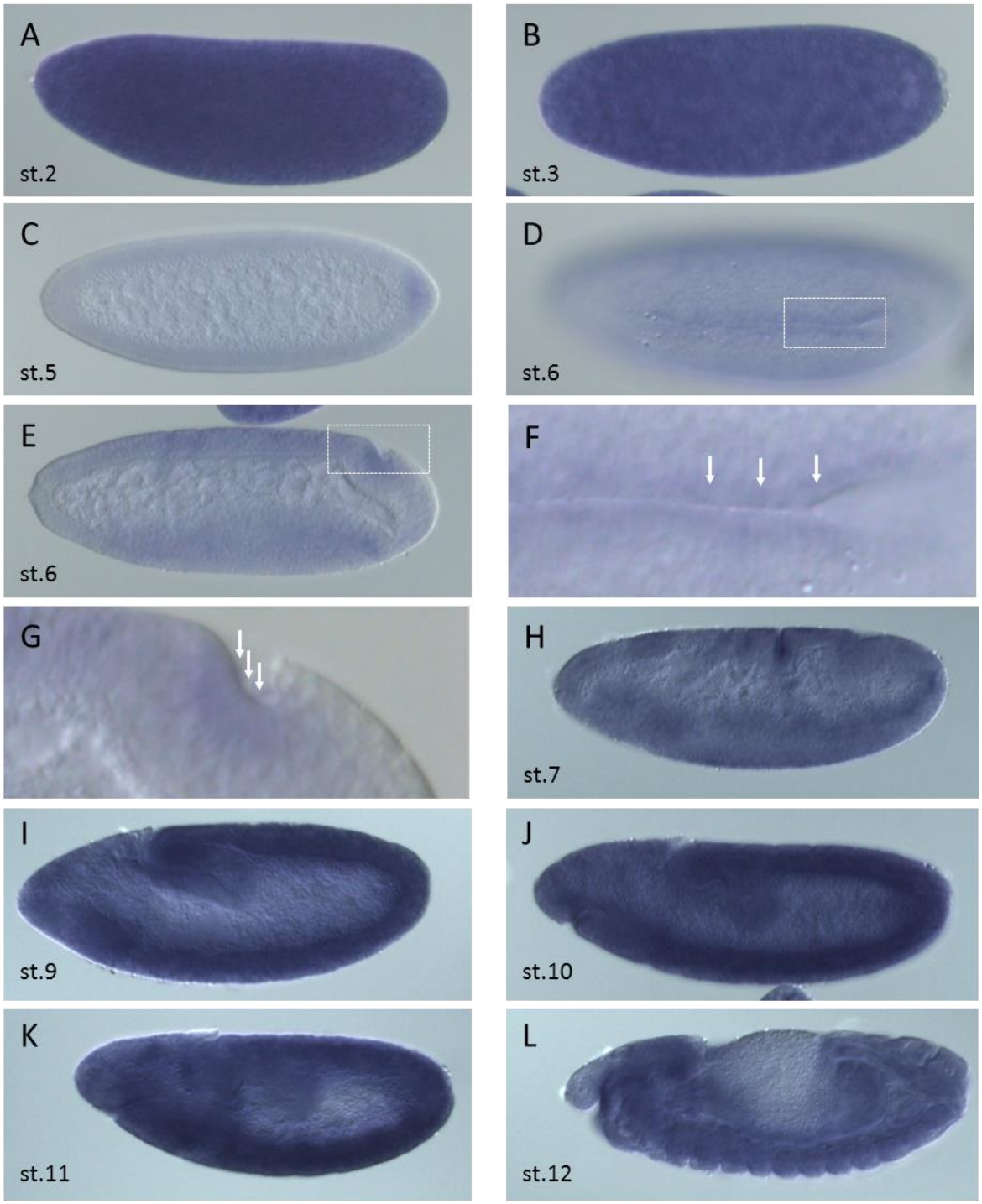

Fig.2

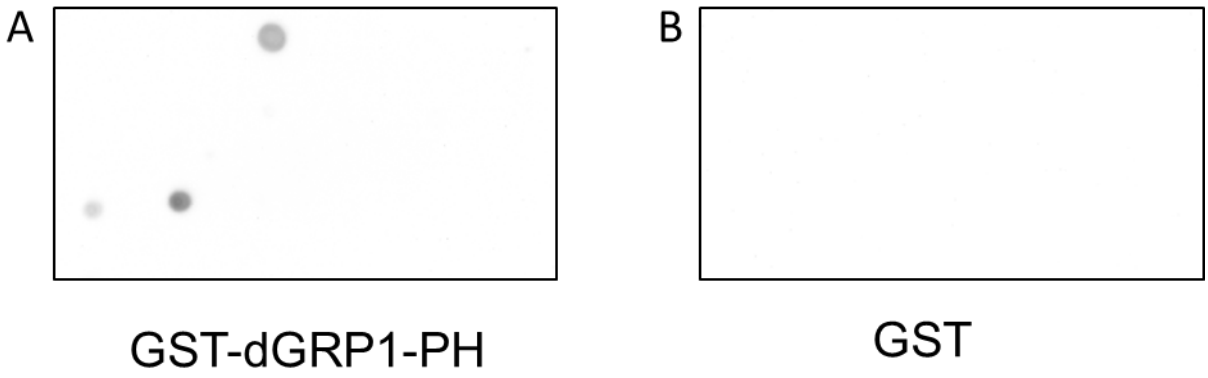
A
B
GST-dGRP1-PH
GST

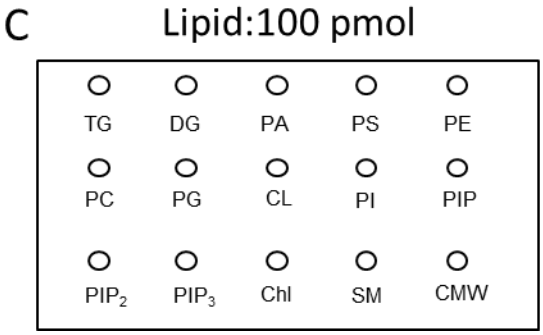
C
Lipid:100 pmol
TG
DG
PA
PS
PE
PC
PG
CL
PI
PIP
PIP2
PIP3
Chl
SM
CMW

Fig.3

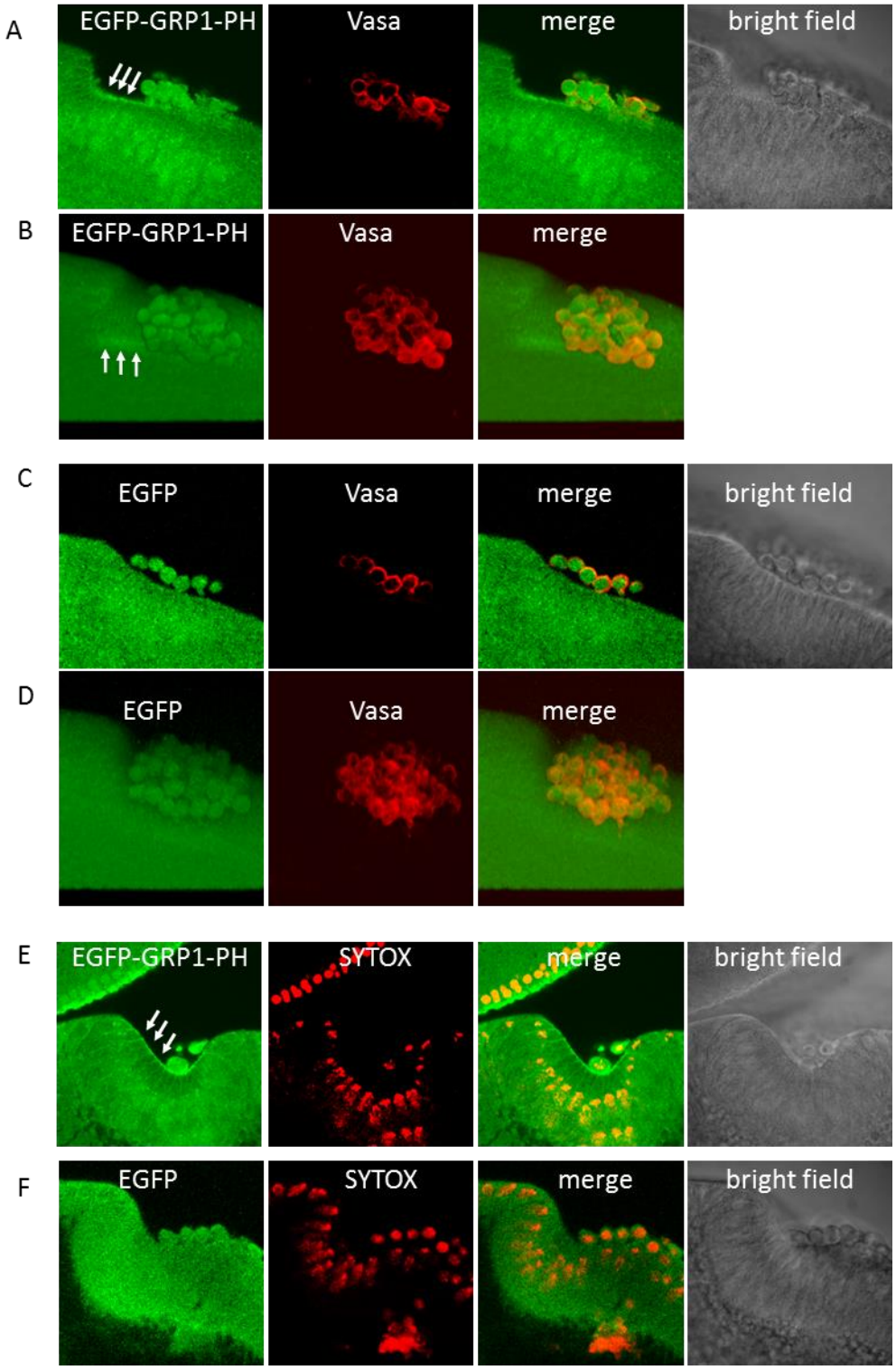
A
EGFP-GRP1-PH
Vasa
merge
bright field
B
EGFP-GRP1-PH
Vasa
merge
C
EGFP
Vasa
merge
bright field
D
EGFP
Vasa
merge
E
EGFP-GRP1-PH
SYTOX
merge
bright field
F
EGFP
SYTOX
merge
bright field

Fig.4

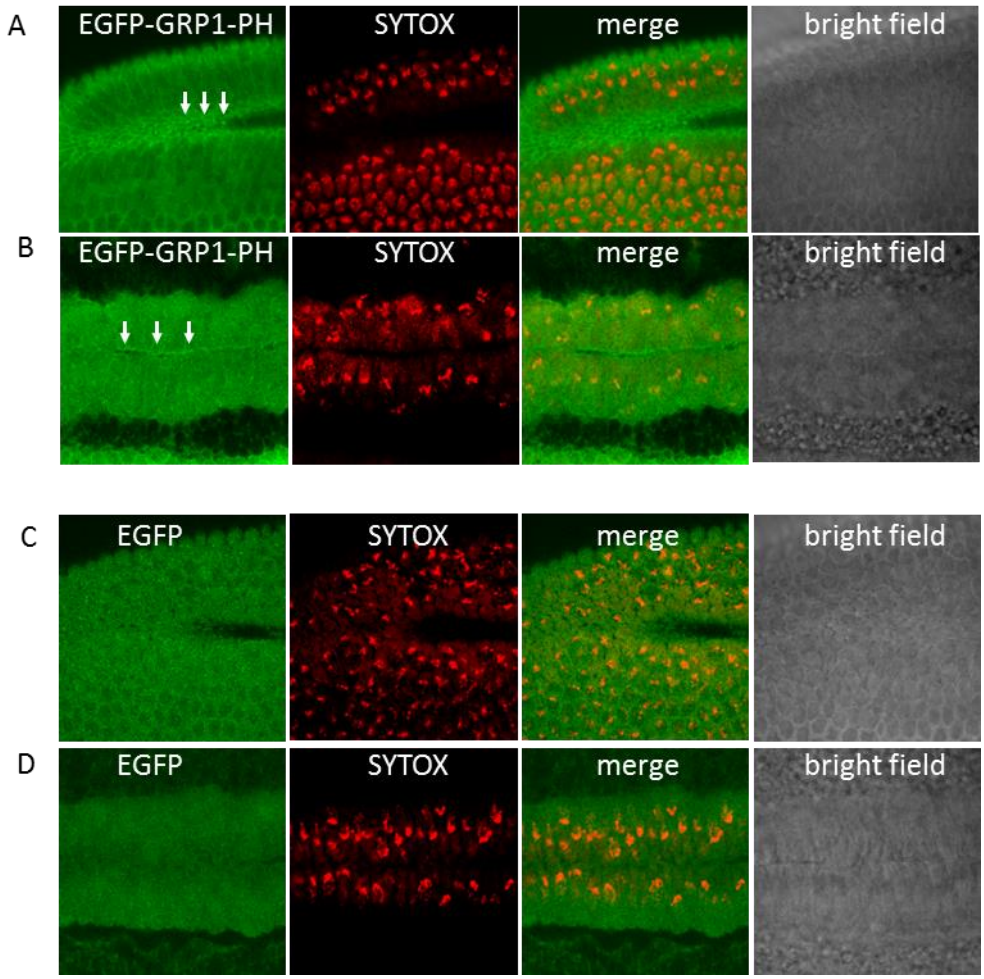
A
EGFP-GRP1-PH
SYTOX
merge
bright field
B
EGFP-GRP1-PH
SYTOX
merge
bright field
C
EGFP
SYTOX
merge
bright field
D
EGFP
SYTOX
merge
bright field

Fig.5

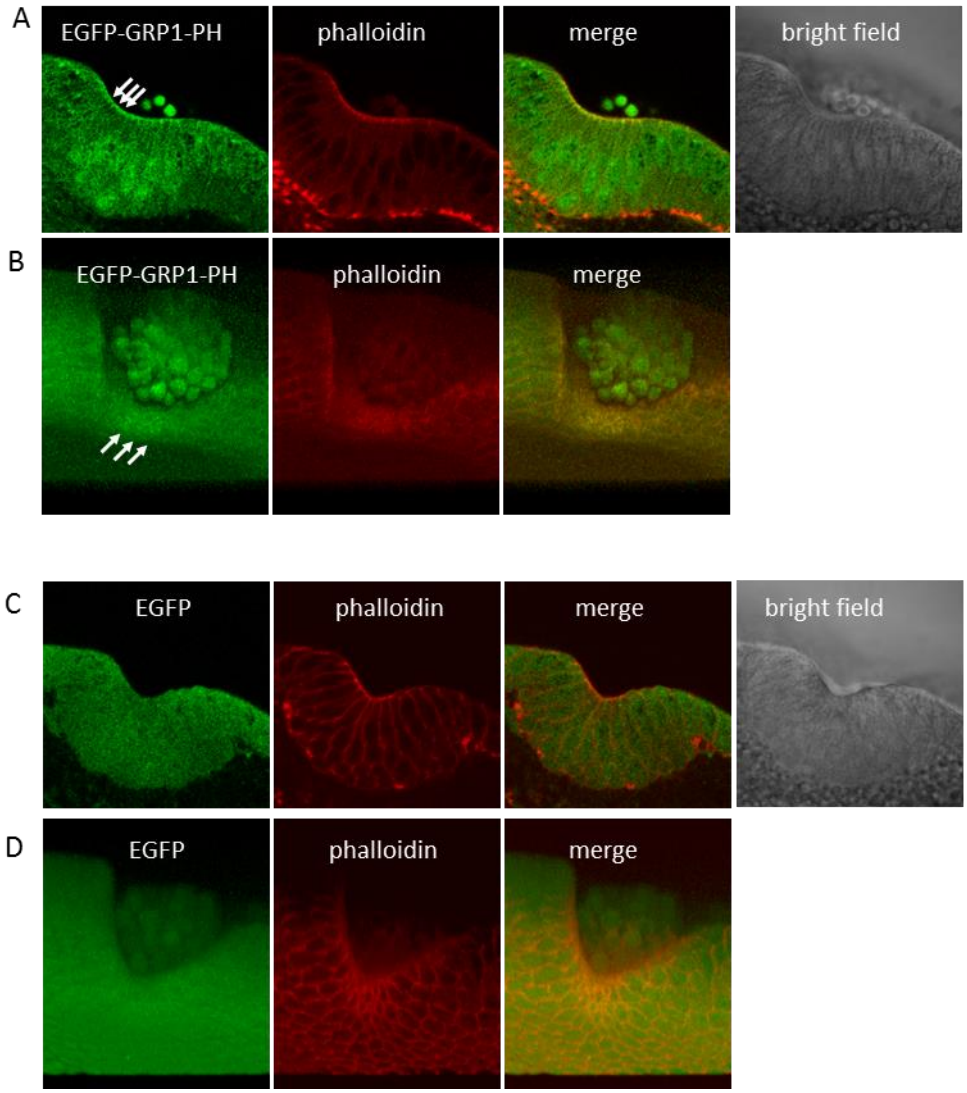
A
EGFP-GRP1-PH
phalloidin
merge
bright field
B
EGFP-GRP1-PH
phalloidin
merge
C
EGFP
phalloidin
merge
bright field
D
EGFP
phalloidin
merge

Fig.6

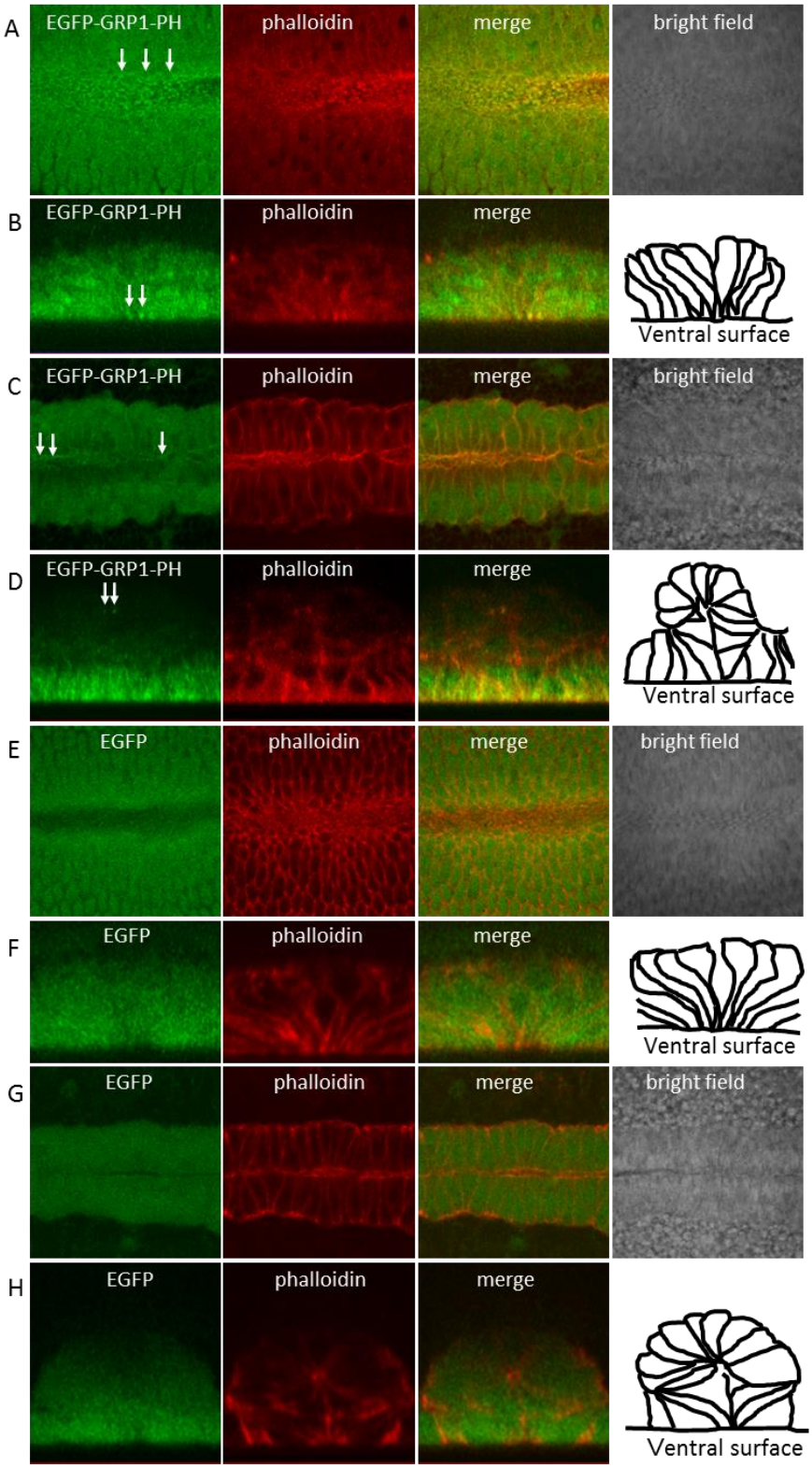
A
EGFP-GRP1-PH
phalloidin
merge
bright field
B
EGFP-GRP1-PH
phalloidin
merge
Ventral surface
C
EGFP-GRP1-PH
phalloidin
merge
bright field
D
EGFP-GRP1-PH
phalloidin
merge
Ventral surface
E
EGFP
phalloidin
merge
bright field
F
EGFP
phalloidin
merge
Ventral surface
G
EGFP
phalloidin
merge
bright field
H
EGFP
phalloidin
merge
Ventral surface

Fig. 7

Submitted Paper

Expression pattern of class I phosphoinositide 3-kinase and distribution of its product phosphatidylinositol-3, 4, 5-trisphosphate during *Drosophila* embryogenesis

（ショウジョウバエの胚発生におけるクラスⅠ ホスホイノシチド 3-キナーゼ及びその産物、ホスファチジルイノシトール-3, 4, 5-三リン酸の発現パターン）

Gene Expression Patterns（投稿中）

著者名： Xin Xi, Kazuaki Tatei, Yumiko Kihara, Takashi Izumi